J|A|C|S
ARTICLES
Published on Web 12/19/2003

Facile Ring Opening of Iron(III) and Iron(II) Complexes of *meso*-Amino-octaethylporphyrin by Dioxygen

Sankar Prasad Rath,† Heather Kalish,† Lechosław Latos-Grażyński,*,‡ Marilyn M. Olmstead,† and Alan L. Balch*,†

Contribution from the Department of Chemistry, University of California, Davis, California 95616, and Department of Chemistry, University of Wrocław, Wrocław, Poland

Received September 10, 2003; E-mail: albach@ucdavis.edu

Abstract: Pyridine solutions of ClFe^{III}(*meso*-NH_2-OEP) undergo oxidative ring opening when exposed to dioxygen. The high-spin iron(III) complex, ClFe^{III}(*meso*-NH_2-OEP), has been isolated and characterized by X-ray crystallography. In the solid state, it has a five-coordinate structure typical for high-spin ($S = {}^5/_2$) iron(III) complex. In chloroform-*d* solution, ClFe^{III}(*meso*-NH_2-OEP) displays an ^{1}H NMR spectrum characteristic of a high-spin, five-coordinate complex and is unreactive toward dioxygen. However, in pyridine-d_5 solution a temperature-dependent equilibrium exists between the high-spin ($S = {}^5/_2$), six-coordinate complex, {(py)ClFe^{III}(*meso*-NH_2-OEP)}, and the six-coordinate, low spin ($S = {}^1/_2$ with the less common $(d_{xz}d_{yz})^4(d_{xy})^1$ ground state)) complex, [$(py)_2$Fe^{III}(*meso*-NH_2-OEP)]$^+$. Such pyridine solutions are air-sensitive, and the remarkable degradation has been monitored by ^{1}H NMR spectroscopy. These studies reveal a stepwise conversion of ClFe^{III}(*meso*-NH_2-OEP) into an open-chain tetrapyrrole complex in which the original amino group and the attached meso carbon atom have been converted into a nitrile group. Additional oxidation at an adjacent meso carbon occurs to produce a ligand that binds iron by three pyrrole nitrogen atoms and the oxygen atom introduced at a meso carbon. This open-chain tetrapyrrole complex itself is sensitive to attack by dioxygen and is converted into a tripyrrole complex that is stable to further oxidation and has been isolated. The process of oxidation of the Fe(III) complex, ClFe^{III}(*meso*-NH_2-OEP), is compared with that of the iron(II) complex, $(py)_2$Fe^{II}(*meso*-NH_2-OEP); both converge to form identical products.

Introduction

We recently reported that pyridine solutions of $(py)_2$Fe^{II}(*meso*-NH_2-OEP), **1**, are unusually reactive toward exposure to atmospheric dioxygen.[1] While solutions of $(py)_2$Fe^{II}(OEP) retain their initial red color after hours of exposure to dioxygen, a red solution of $(py)_2$Fe^{II}(*meso*-NH_2-OEP) in pyridine immediately turns green when exposed to dioxygen, and a process of heme cleavage begins which occurs in several stages over a period of a day. The process is accompanied by the cleavage of the heme ring as shown in Scheme 1. The initial reaction with dioxygen produces a green intermediate, **2**, which has been identified by its remarkable paramagnetically shifted ^{1}H NMR spectrum that shows methylene resonances in the upfield and downfield regions.[1,2] The structures shown in Scheme 1 have been proposed for this intermediate, which undergoes further reaction with dioxygen over a period of hours to form the open-chain tetrapyrrole complex **3**. Complex **3** has been isolated and characterized by single-crystal X-ray diffraction.[1]

Scheme 1

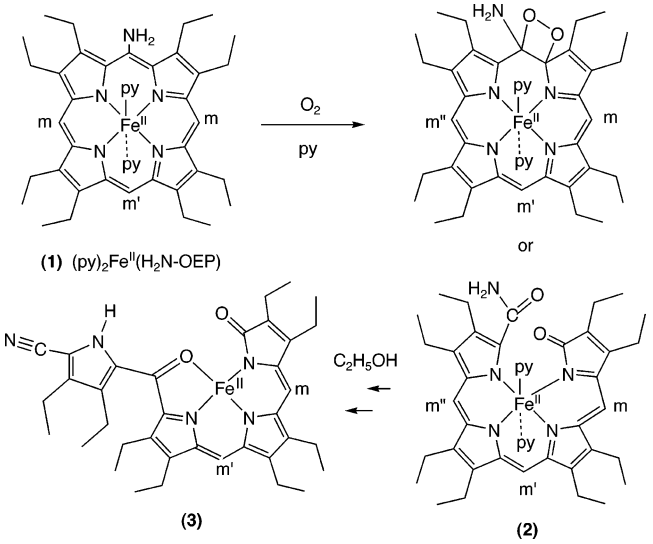

The process shown in Scheme 1 is distinct from coupled oxidation, a procedure shown in Scheme 2 in which a heme or heme protein is cleaved using both an oxidant, dioxygen, and

† University of California.
‡ University of Wrocław.

(1) Kalish, H.; Lee, H. M.; Olmstead, M. M.; Latos-Grażyński, L.; Rath, S. P.; Balch, A. L. *J. Am. Chem. Soc.* **2003**, *125*, 4674.

(2) For a discussion of the electronic structure of such tetrapyrroles see; Szterenberg, L.; Latos-Grażyński, L.; Wojaczyński, *ChemPhysChem*. **2003**, *4*, 691. The present paper does not contain new information in regard to the structure of this green intermediate. The structures shown for (**2**) in Scheme 1 are consistent with the ^{1}H NMR data but should not be considered as definitive. Further work to determine the structure of this green intermediate is in progress.

10.1021/ja0384431 CCC: $27.50

Scheme 2

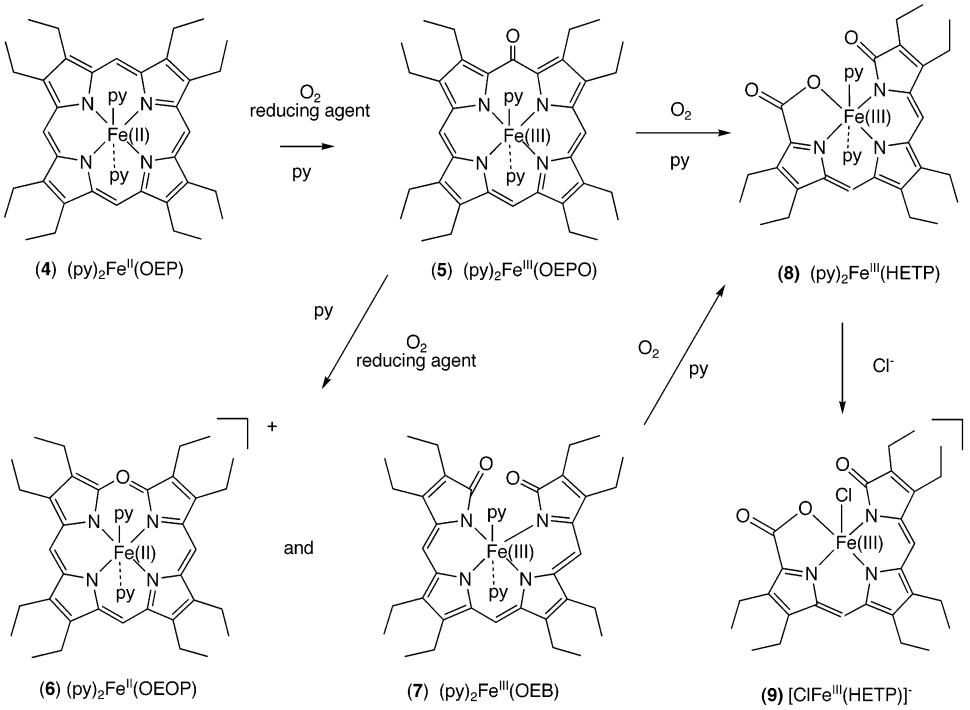

a reducing agent, generally hydrazine or ascorbic acid.[3−6] The products of coupled oxidation of $(py)_2Fe^{II}$(OEP), **4**, are the verdoheme, $[(py)_2Fe^{II}(OEOP)]^+$, **6**,[7] and an iron(III) complex of octaethylbiliverdin, $(py)_2Fe^{II}$(OEB), **7**.[8] The oxophlorin complex, $(py)_2Fe^{III}$(OEPO), **5**,[9] and analogues with hydrazine as axial ligands, are intermediates in the process, and procedures for the isolation and crystallographic characterization of **5** have been devised.[10] The green-brown complex $(py)_2Fe^{III}$(OEPO), **5**, itself is very sensitive toward dioxygen. Exposure of a pyridine solution of $(py)_2Fe^{III}$(OEPO), **5**, to dioxygen results in its conversion into the hexaethyltripyrrole complex, $[(py)_2Fe^{III}(HETP)]$, **8**, as seen in Scheme 2.[11]

Here we report detailed characterization of the high-spin, five-coordinate iron(III) complex, $ClFe^{III}$(*meso*-NH_2-OEP), **10**, and demonstrate that it is also attacked by dioxygen when dissolved in pyridine solution. Comparisons are made between the processes of oxidation of the iron(II) complex, $(py)_2Fe^{II}$(*meso*-NH_2-OEP), and the iron(III) complex, $ClFe^{III}$(*meso*-NH_2-OEP).

Results

A sample of *meso*-NH_2-H_2OEP was prepared by the reduction of *meso*-NO_2-H_2OEP with tin and hydrochloric acid by a previously developed route,[12] and iron was inserted to produce $ClFe^{III}$(*meso*-NH_2-OEP), **10**. The UV/vis spectrum of this complex is given in the Experimental Section and is similar to those of other high-spin, five coordinate Fe(III) porphyrins.

Crystallographic Characterization of $ClFe^{III}$(*meso*-NH_2-OEP), 10. The structure of $ClFe^{III}$(*meso*-NH_2-OEP) has been determined by X-ray crystallography. Figure 1 shows a drawing of the molecule. Selected interatomic distances and angles are given in the figure caption. The complex has a five-coordinate structure typical for high-spin ($S = {}^5/_2$) iron(III) complexes with Fe−N bond distances that fall near the range (2.060−2.087 Å) found for this type of porphyrin complex.[13] The Fe−N distances, which range from 2.054(2) to 2.080(2) Å, and the Fe−Cl distance, 2.2576(8) Å, are similar to those in $ClFe^{III}$(OEP) (in C_{60}·$ClFe^{III}(OEP)$·$CHCl_3$),[14] $ClFe^{III}$(*meso*-O_2N-OEP),[15] $ClFe^{III}$(*meso*-CH_3COO-OEP),[16] $ClFe^{III}$(*meso*-Ph-OEP),[17] and $ClFe^{III}$(*meso*-NCOEP).[17] The iron atom is 0.45 Å from the N_4 plane, a distance which is in the range (0.39−0.54 Å) seen for other high-spin, five-coordinate iron(III) porphyrin complexes.[13]

Molecules of $ClFe^{III}$(*meso*-NH_2-OEP) pack about centers of symmetry as shown in Figure 2. This arrangement allows hydrogen bonding to occur between the amino group of one molecule and the axial chloride ligand of the other. The Cl···N distance is 3.088(3) Å. While a number of meso-substituted complexes of octaethylporphyrin with small substituents display disorder in the position of that meso group in the solid state,[18,19]

(3) Warburg, O.; Negelein, E. *Chem. Ber.* **1930**, *63*, 1816.
(4) St Claire, T. N.; Balch, A. L. *Inorg. Chem.* **1999**, *38*, 684.
(5) Hildebrand, D. P.; Tang, H.; Luo, Y.; Hunter, C. L.; Smith, M.; Brayer, G. D.; Mauk, A. G. *J. Am. Chem. Soc.* **1996**, *118*, 12909.
(6) Avila, L.; Huang, H.; Damaso, C. O.; Lu, S.; Moënne-Loccoz, P.; Rivera, M. *J. Am. Chem. Soc.* **2003**, *125*, 4103.
(7) Balch, A. L.; Koerner, R.; Olmstead, M. M. *J. Chem. Soc., Chem. Commun.* **1995**, 873.
(8) Balch, A. L.; Latos-Grażyński, L.; Noll, B. C.; Olmstead, M. M.; Safari, N. *J. Am. Chem. Soc.* **1993**, *115*, 9056.
(9) The electronic structure of this compound is complicated and can involve several distributions of electrons between the metal and the ligand: see Balch, A. L. *Coord. Chem. Rev.* **2000**, *200−202*, 349. Here, for simplicity we limit ourselves to one possible structure involving Fe(III) and a trianionic ligand.
(10) Balch, A. L.; Koerner, R.; Latos-Grażyński, L.; Noll, B. C. *J. Am. Chem. Soc.* **1996**, *118*, 2760.
(11) Rath, S. P.; Latos-Grażyński, L.; Olmstead, M. M.; Balch, A. L. *J. Am. Chem. Soc.* **2003**, *125*, 12678.
(12) Bonnett, R.; Stephenson, G. F. *J. Org. Chem.* **1965**, *30*, 2791.
(13) Scheidt, R. W.; Reed, C. A. *Chem. Rev.* **1981**, *81*, 543.
(14) Olmstead, M. M.; Costa, D. A.; Maitra, K.; Noll, B. C.; Phillips, S. L.; Van Calcar, P. M.; Balch, A. L. *J. Am. Chem. Soc.* **1999**, *121*, 7090.
(15) Senge, M. Personal communication. CCD file, TOYSAB.
(16) Balch, A. L.; Latos-Grażyński, L.; Noll, B. C.; Olmstead, M. M.; Zovinka, E. P. *Inorg. Chem.* **1992**, *31*, 2248.
(17) Kalish, H.; Camp, J. E.; Stępién, M.; Latos-Grażyński, L.; Olmstead, M. M.; Balch, A. L. *Inorg. Chem.* **2002**, *41*, 989.
(18) Examples include $ClFe^{III}$(*meso*-NC-OEP),[17] $(py)_2Fe$(OEPO),[7] and Zn^{II}-(OEPO•).[19]

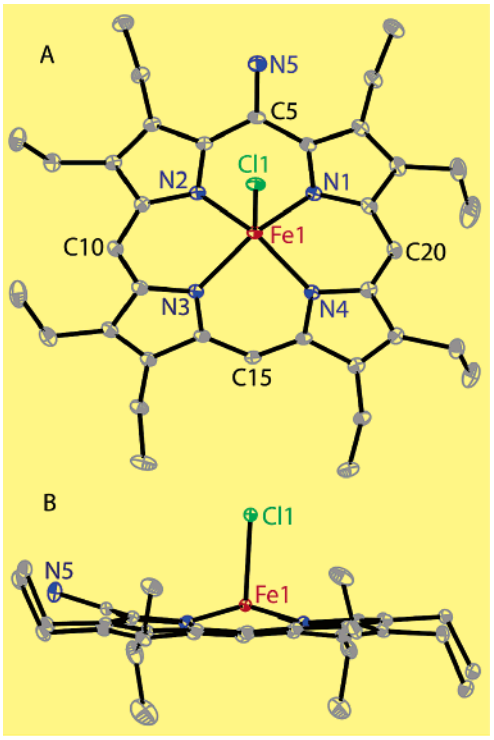

Figure 1. Two perspective views of ClFe^{III}(*meso*-NH$_2$-OEP) showing 30% thermal contours. Selected bond distances: Fe1−N1, 2.076(2); Fe1−N2, 2.080(2); Fe1−N3, 2.054(2); Fe1−N4, 2.056(2); Fe1−Cl, 2.2596(8); N5−C5, 1.352(4) Å. Selected bond angles: N1−Fe−N2, 85.47(9); N1−Fe−N3, 154.77(9); N1−Fe−N4, 88.51(9); N2−Fe−N3, 88.40(9); N2−Fe−N4, 154.39(9); N3−Fe−N4, 86.53(9); Cl−Fe−N1, 103.51(7); Cl−Fe−N2, 105.44(6); Cl−Fe−N3, 101.71(6); Cl−Fe−N4, 100.17(6)°.

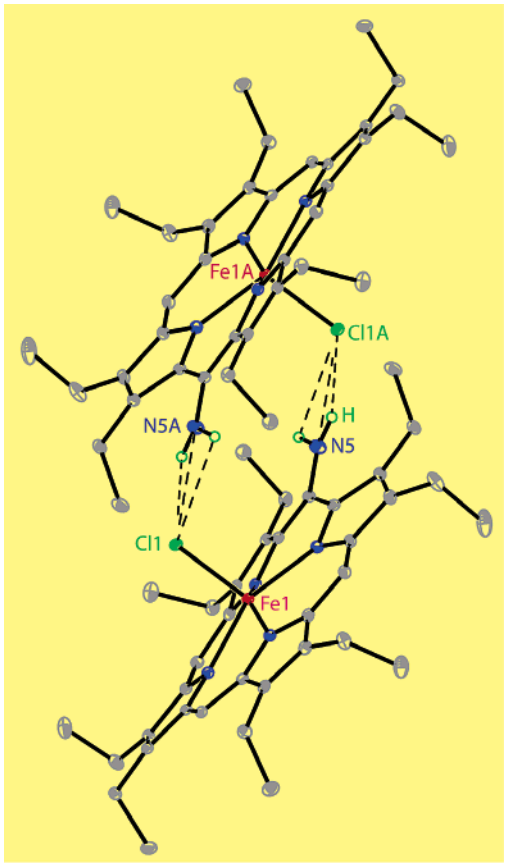

Figure 2. A view of two molecules of ClFe^{III}(*meso*-NH$_2$-OEP) which shows the hydrogen bonding interactions between the chloro and amino groups.

that is not the case here. The hydrogen bonding to the adjacent axial chloride ligands provides the requisite organization in the crystal. A number of other cases where hydrogen bonding is associated with the ordering of the location of small meso substituents in octaethylporphyrin-derived complexes are known.[20,21]

The porphyrin ring in ClFe^{III}(*meso*-NH$_2$-OEP) is unusually distorted. This is best appreciated by turning to Figure 3 where the out-of-plane displacements in units of 0.01 Å of the core atoms of ClFe^{III}(*meso*-NH$_2$-OEP) are compared with those of ClFe^{III}(OEP), ClFe^{III}(*meso*-NC-OEP), and ClFe^{III}(*meso*-O$_2$N-OEP). Porphyrin distortions from planarity follow the low-frequency, normal vibrational modes of the porphyrin macrocycle and can involve *sad*, *ruf*, *dom*, *wav*(*x*), *wav*(*y*) and *pro* deformations.[22,23] In ClFe^{III}(*meso*-NH$_2$-OEP) the porphyrin core assumes a *ruf* conformation rather than the *dom* conformation found for the parent, ClFe^{III}(OEP).[24] The *ruf* distortion in ClFe^{III}(*meso*-NH$_2$-OEP) is similar to that in ClFe^{III}(*meso*-NC-OEP), but the out-of-plane displacements are much greater for the former. Earlier we noted that "for the most part, the mono-meso-substituted complexes showed smaller out-of-plane atom displacements for the porphyrin core atoms than is observed for the unsubstituted parent, ClFe^{III}(OEP)".[17] That statement is certainly not appropriate for ClFe^{III}(*meso*-NH$_2$-OEP) which shows the largest out-of-plane displacements. The largest of these displacements occurs in the vicinity of the amino group. These displacements may be caused by the need to accommodate this substituent and by the hydrogen bonding shown in Figure 2. Note that the amino group is pulled out of the porphyrin plane in the direction of the chloride ligand of the neighboring ClFe^{III}(*meso*-NH$_2$-OEP) molecule.

^{1}H NMR Spectra of ClFe^{III}(*meso*-NH$_2$-OEP) in Solution. The ^{1}H NMR spectrum of ClFe^{III}(*meso*-NH$_2$-OEP) in chloroform-*d* at 298 K is shown in Figure 4. The idealized C_s symmetry expected for ClFe^{III}(*meso*-NH$_2$-OEP) in solution suggests that there should be two meso resonances in a 2:1 intensity ratio, a single amino proton resonance, eight equally intense methylene resonances, and four equally intense methyl resonances for five-coordinate complexes. The eight methylene resonances arise from the diastereotopic nature of these protons which occurs whenever the two sides of the porphyrin are inequivalent. As seen in Figure 4, there are two resonances in the far upfield region with a 2:1 intensity ratio that can be assigned to the meso protons, and seven resonances, one with twice the intensity of the other seven in the downfield region that can be assigned to the methylene protons. The resonance at 14 ppm is assigned to the amino protons. This assignment has been confirmed by shaking the sample with D$_2$O which results in the disappearance of this resonance. The position of the amino resonance resembles that of ClFe^{III}(2-NH$_2$-TPP).[25]

(19) Balch, A. L.; Noll, B. C.; Zovinka, E. P. *J. Am. Chem. Soc*. **1991**, *114*, 3380.
(20) Examples include (py)Zn^{II}(OEPOH···py)[19] and [BrFe^{III}(OEPO···HCCl$_3$).[21]
(21) Balch, A. L.; Latos-Grażyński, L.; Noll, B. C.; Szterenberg, L.; Zovinka, E. P. *J. Am. Chem. Soc*. **1993** , *115*, 11846.
(22) Jentzen, W.; Song, X.-Z.; Shelnutt, J. A. *J. Phys. Chem. B* **1997**, *101*, 1684.
(23) Shelnutt, J. A.; Song, X.-Z.; Ma, J.-G.; Jia, S.-L.; Jentzen, W.; Medforth, C. J. *Chem. Soc. Rev.* **1998**, *27*, 31.
(24) Scheidt, W. R.; Finnegan, M. G. *Acta Crystallogr*. **1989**, *C45*, 1214.
(25) Wojaczyński, J.; Latos-Grażyński, L.; Hrycyk, W.; Pacholska, E.; Rachlewicz, K.; Szterenberg, L. *Inorg. Chem*. **1996**, *35*, 6861.

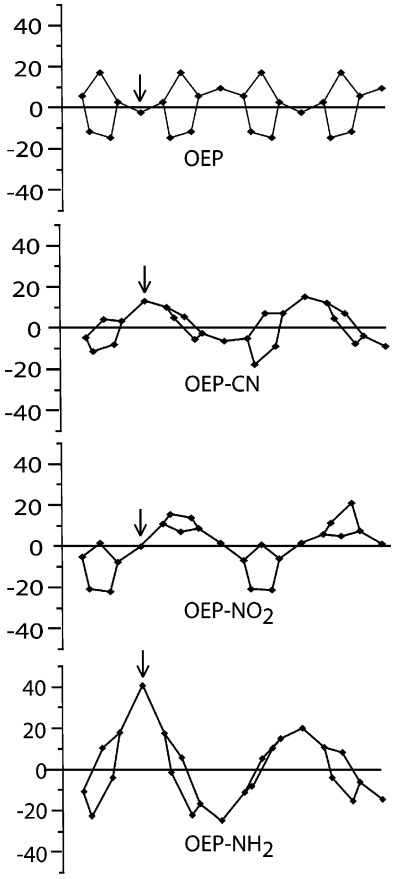

Figure 3. Diagrams comparing the out-of-plane displacements in units of 0.01 Å for the porphyrin core atoms from the mean plane of the porphyrin for ClFe^{III}(OEP), ClFe^{III}(*meso*-NC-OEP), and ClFe^{III}(*meso*-NO_2-OEP), and ClFe^{III}(*meso*-NH_2-OEP). The meso substituents are attached to the carbon atoms denoted by arrows.

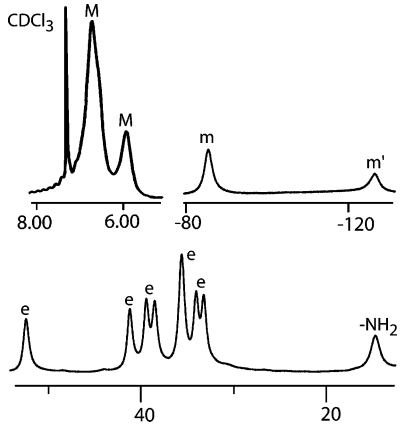

Figure 4. Portions of the 500 MHz ^{1}H NMR spectrum of ClFe^{III}(*meso*-NH_2-OEP) in chloroform-*d* at 25 °C. Resonances are labeled m and m′ for the meso protons, M for methyl protons, and e for the methylene protons.

The two resonances with a 3:1 relative intensity ratio are assigned to the methyl protons. This pattern of resonances is entirely consistent with the spectral features seen earlier for other complexes of the type ClFe^{III}(*meso*-R-OEP).[17] Chloroform solutions of ClFe^{III}(*meso*-NH_2-OEP) are stable to exposure to dioxygen.

However, pyridine solutions of ClFe^{III}(*meso*-NH_2-OEP) are unstable in the presence of dioxygen. To examine the nature of the oxidation process, we begin by examining the ^{1}H NMR behavior of ClFe^{III}(*meso*-NH_2-OEP) in pyridine-d_5 solution in

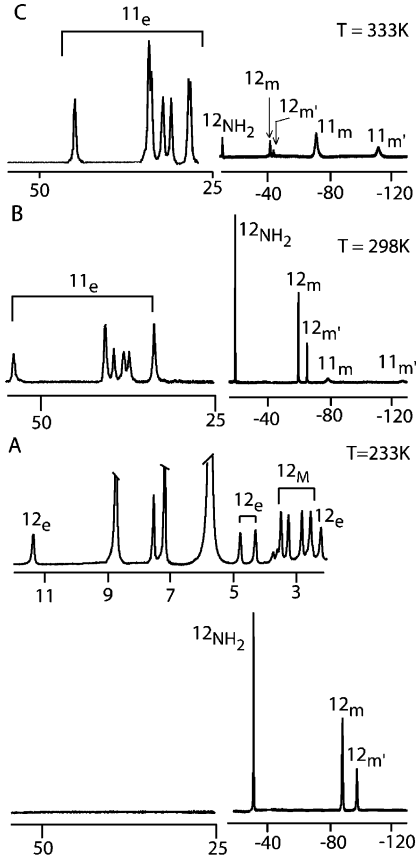

Figure 5. In pyridine-d_5, 500 MHz ^{1}H NMR spectra of ClFe^{III}(*meso*-NH_2-OEP) at A, 233; B, 298; and C, 333 K. Resonances due to $(py)_n$ClFe^{III}(*meso*-NH_2-OEP) are labeled **11**, while those of $[(py)_2Fe^{III}$(*meso*-NH_2-OEP)$]^+$ are labeled **12**. Subscripts m and m′ denote the meso protons, M denotes the methyl protons, e denotes the methylene protons, and NH_2 denotes the amino protons. In traces A and B, the vertical scales in the upfield and downfield region have been independently adjusted to allow the individual resonances to be seen.

the absence of dioxygen. Relevant ^{1}H NMR spectra at three different temperatures are shown in Figure 5. The spectra are best understood in comparison to the spectra previously observed for other complexes of the type ClFe^{III}(*meso*-R-OEP) in pyridine-d_5 solution.[17] For example ClFe^{III}(*meso*-*n*-Bu-OEP) in pyridine-d_5 solution at 298 K shows a spectrum with two meso resonances in the far upfield region at −50.70 and −63.51 ppm and seven methylene resonances (one with twice the intensity of the other six) in the region 47−34 ppm.[17] In comparison, the spectrum of ClFe^{III}(*meso*-NH_2-OEP) in pyridine-d_5 solution is more complex. As seen in Trace B of Figure 5, this spectrum shows resonances due to two different species. The resonances of these two species are labeled **11** and **12**, and as seen in Figure 5, the relative intensities of the two different species change with changes in temperature. At high temperature, species **11** dominates, while at low temperature, **12** is the major species. The pattern of resonances observed for species **11** resembles that reported for ClFe^{III}(*meso*-*n*-Bu-OEP) in pyridine-d_5 solution[17] with two meso resonances in the upfield region at −79 and −130 ppm and a set of six methylene resonances (two with twice the intensity of the other four) in the downfield region between 35 and 55 ppm. As in the case of ClFe^{III}(*meso*-*n*-Bu-OEP) in pyridine-d_5 solution, we assign these resonances to the high-spin complexes that are involved in the dynamic equilibrium shown in reaction 1.[17] We will refer to the species

present in this dynamic equilibrium as $(py)_n ClFe^{III}$(*meso*-NH_2-OEP) where $n = 0$ or 1. Some examples of mixed ligand complexes of iron(III) porphyrins such as high-spin {(py)(SCN)Fe^{III}(OEPO)} have been isolated.[26,27]

$$ClFe^{III}(meso\text{-R-OEP}) + py \rightleftharpoons (py)ClFe^{III}(meso\text{-R-OEP}) \quad (1)$$

The resonance pattern of species **12** is readily apparent in the spectrum obtained at 233 K that is shown in Trace A of Figure 5. The two resonances at −88.5 and −97.9 ppm with a 2:1 intensity ratio are assigned to the meso protons, while the resonance at −30.9 is assigned to the *meso*-NH_2 protons. When the sample of $ClFe^{III}$(*meso*-NH_2-OEP) is deuterated by exposure to D_2O before dissolution in pyridine, the resonance at −30.9 ppm vanishes. There are no resonances in the downfield region below 12 ppm. Rather four equally intense resonances at 11.3, 4.8, 4.3, and 2.2 ppm, which are shown in the inset to Trace C, are assigned to the methylene resonances. Four equally intense resonances at 3.5, 3.2, 2.8, and 2.5 ppm are assigned to the methyl resonances. This pattern indicates that **12** is a six-coordinate complex with equilivant ligation on either side of the porphyrin ring, since four, rather than eight, methylene resonances are present. Thus, **12** can be identified as the low-spin, six-coordinate complex $[(py)_2Fe^{III}$(*meso*-NH_2-OEP)]Cl. Generally, such six-coordinate complexes are formed by the reactions of pyridine (or substituted pyridines) with $ClFe^{III}$P in methanol solution where the solvent assists in the ionization of the chloride ligand.[28,29] A previous study that examined the ^{1}H NMR spectra of the series of complexes $ClFe^{III}$(*meso*-R-OEP) with R = hydrogen, *n*-butyl, phenyl, chloro, nitrile, nitro, methoxy, and formyl in pyridine-d_5 solution showed that only high-spin species were present.[17]

To further confirm the identity of **12**, we have examined the ^{1}H NMR spectrum of another low-spin, six-coordinate complex, $K[(NC)_2Fe^{III}$(*meso*-NH_2-OEP)]. Solutions of $ClFe^{III}$(*meso*-NH_2-OEP) in methanol-d_4 form the low-spin complex, $K[(NC)_2Fe^{III}$(*meso*-NH_2-OEP)], when potassium cyanide is added. As expected on the basis of symmetry, the spectrum of $K[(NC)_2Fe^{III}$(*meso*-NH_2-OEP)] in methanol-d_4 at 298 K consists of four equally intense methylene resonances at 5.2, 4.7, 4.6, and 3.4 ppm and four equally intense methyl resonances at 3.1, 2.7, 2.6, and 2.5 ppm. These lines are sufficiently narrow so that spin−spin splitting is observed. Each methyl resonance is a triplet, while each methylene resonance is a quartet. The meso protons appear far upfield at −51.7 ppm and −55.5 ppm, and the *meso*-NH_2 resonance appears at 4.3 ppm. The large upfield shifts of the meso protons seen for both $K[(NC)_2Fe^{III}$(*meso*-NH_2-OEP)] and $[(py)_2Fe^{III}$(*meso*-NH_2-OEP)]Cl are entirely consistent with the trend observed previously for low-spin complexes of the type $K[(NC)_2Fe^{III}$(*meso*-R-OEP)].[17] Thus, the presence of electron-donating R substituents results in upfield shifts of the meso proton resonances. This upfield meso proton shift is seen for iron porphyrins with the less common $(d_{xz},d_{yz})^4(d_{xy})^1$ ground state and arises from the presence of spin in the a_{2u}-like porphyrin orbital.[17,26] This orbital has principal contributions at the meso positions and little or no contribution at the pyrrole β-positions. As a consequence, the upfield position of the *meso*-NH_2 resonance seen for $[(py)_2Fe^{III}$(*meso*-NH_2-OEP)]Cl can be atributed to the positive spin density at the meso N atom which is congugated with the π-system of the porphyrin.[25]

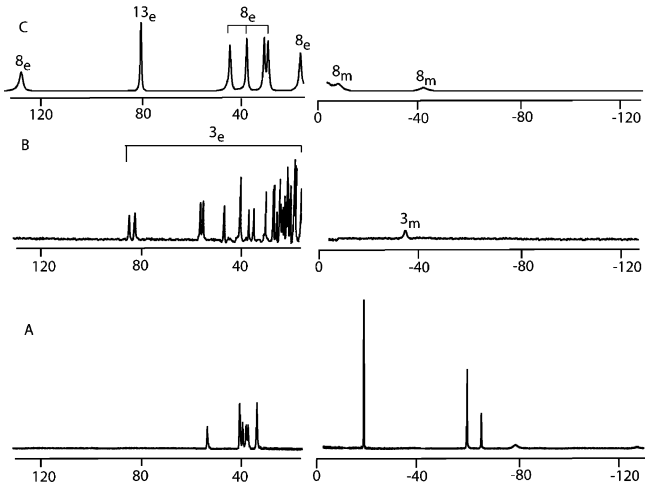

Figure 6. In pyridine-d_5, 500 MHz ^{1}H NMR spectra of the reaction of $ClFe^{III}$(*meso*-NH_2-OEP) at 25 °C with dioxygen: (A) before addition of dioxygen; (B) 12 h after the addition of dioxygen; (C) one week after the addition of dioxygen. Resonances of the open chain tetrapyrrole **3** are labeled 3, those of the tripyrrole complex $(py)_2Fe^{III}$(HETP) **8** are labeled 8, and those of compound **13** are labeled 13. Subscripts m and m′ denote the meso protons, M denotes the methyl protons, e denotes the methylene protons, and NH_2 denotes the amino protons.

^{1}H NMR Spectroscopic Study of the Oxidation of the Iron(III) Complex $ClFe^{III}$(*meso*-NH_2-OEP) in Pyridine Solution. Figure 6 shows ^{1}H NMR spectra of a solution of $ClFe^{III}$(*meso*-NH_2-OEP) in pyridine-d_5 at 298 K before and after addition of dioxygen Trace A shows the spectrum before the addition of dioxygen. Trace B shows the spectrum 12 h after the addition of dioxygen. The resonances of $(py)_n ClFe^{III}$(*meso*-NH_2-OEP) ($n = 0$, 1) and $[(py)_2Fe^{III}$(*meso*-NH_2-OEP)]Cl have vanished. They are replaced by a new set of resonances due to the previously characterized,[1] open-chain tetrapyrrole complex **3** shown in Scheme 1. Further exposure to dioxygen over a period of one week results in the loss of the resonances of **3** and the growth of new resonances as seen in Trace C of Figure 6. In Trace C two sets of resonances have been identified. Those labeled 8 are due to the presence of $[py)_2Fe^{III}$(HETP)], **8**, (see Scheme 2) whose ^{1}H NMR spectrum has been reported earlier.[11] The prominent resonance at 81.2 ppm signals the presence of another complex, **13** (vide infra).

^{1}H NMR Spectroscopic Study of the Oxidation of $(py)_2Fe^{II}$(*meso*-NH_2-OEP) in Pyridine Solution. Figure 7 shows the effects of dioxygen addition on the ^{1}H NMR spectra of a solution of $(py)_2Fe^{II}$(*meso*-NH_2-OEP) in pyridine-d_5 at 298 K. Trace A shows the spectrum before the addition of dioxygen. No resonances occur outside the 0 to 10 ppm region that is shown, because the starting complex is diamagnetic. Immediately upon exposure to dioxygen, the spectrum of the complex is transformed into that shown in Trace B of Figure 7. At this point new resonances of a green intermediate **2** are present. But after 20 min exposure to dioxygen the spectrum shown in Trace C is obtained. At this point a number of new resonances are present along with those of the green intermediate

(26) Adams, K. M.; Rasmussen, P. G.; Scheidt, W. R.; Hatano, K. *Inorg. Chem.* **1979**, *18*, 1892.
(27) Scheidt, W. R.; Lee, Y. J.; Geiger, D. K.; Taylor, K.; Hatano, K. *J. Am. Chem. Soc.* **1982**, *104*, 3367.
(28) Walker, F. A.; Lo, M.; Ree, M. T. *J. Am. Chem. Soc.* 1**976**, *98*, 5552.
(29) Satterlee, J. D.; La Mar, G. N.; Frye, J. S. *J. Am. Chem. Soc.* **1976**, *98*, 7275.

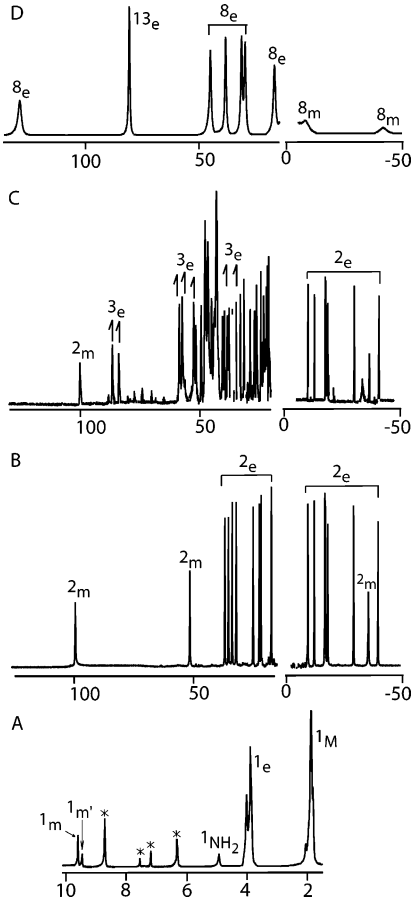

Figure 7. In pyridine-d_5, 500 MHz ^{1}H NMR spectra of the reaction of (py)$_2$Fe^{II}(*meso*-NH$_2$-OEP) at 25 °C with dioxygen: (A) before addition of dioxygen; since the sample is diamagentic there are no resonances outside the 0 to 10 ppm window; (B) 2 min after the addition of dioxygen; (C) 20 min after the addition of dioxygen; (D) one week after the addition of dioxygen. Resonances due to the green intermediate **2** are labeled 2. Those of the open chain tetrapyrrole complex **3** are labeled 3, while those of complexes **8** and **13** are labeled 8 and 13. Subscripts m and m′ denote the meso protons, M denotes the methyl protons, e denotes the methylene protons, and NH$_2$ denotes the amino protons.

2. The resonances of the open-chain tetrapyrrole complex **3** are clearly present along with others. Further exposure to dioxygen over a period of a week produces the spectrum shown in Trace D of Figure 7. At this point the resonances of the open-chain tetrapyrrole complex **3** have vanished. New resonances due to [(py)$_2$Fe^{III}(HETP)], **8**,[10] are clearly observed as is a resonance at 81.2 ppm due to **13**. The spectrum shown in Trace D of Figure 7 resembles that shown in Trace C of Figure 6. Thus, oxidation of either (py)$_2$Fe^{II}(*meso*-NH$_2$-OEP) or ClFe^{III}(*meso*-NH$_2$-OEP) in pyridine yields the same products, **8** and **13**, in the same ratio.

Crystallographic and Spectroscopic Characterization of the Open-Chain Tetrapyrrole Complex 3. The open-chain tetrapyrrole complex **3** has been isolated from oxidized pyridine solutions of ClFe^{III}(*meso*-NH$_2$-OEP) by precipitation with ethanol. The structure of the product as determined by X-ray crystallography was reported briefly in a communication.[1] Two different molecules are present in the crystalline solid. One, which is shown in Figure 8, is five-coordinate with an axial ethanol ligand, while the other is four-coordinate and lacks the ethanol ligand. Selected interatomic distances and angles for the five-coordinate complex are given in the caption for Figure

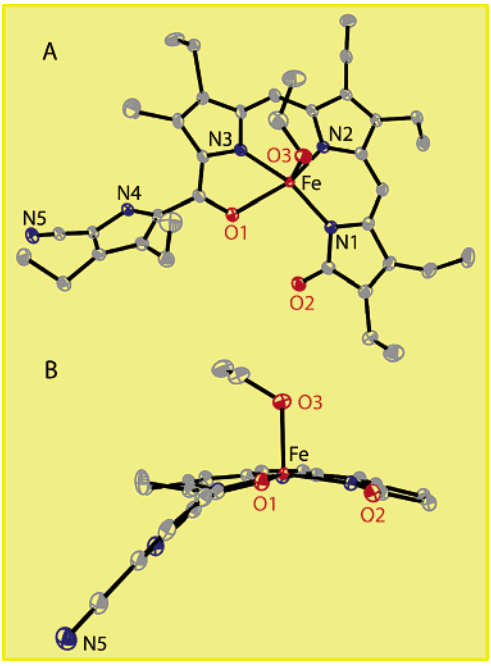

Figure 8. Two perspective views of the open chain tetrapyrrole complex **3** showing 30% thermal contours. The crystal contains two independent molecules, the one with a coordinated axial ethanol ligand is shown here. For clarity the ethyl groups have been removed in part B. Selected bond distances: Fe1−N1, 1.984(2); Fe1−N2, 2.040(2); Fe1−N3, 2.011(2); Fe1−O1, 2.3155(19); Fe1−O3, 2.111(2); O1−C15, 1.250(3); O2−C1, 1.249(3); O3−C37, 1.451(4); N5−C20, 1.151(4) Å. Selected bond angles: N1−Fe1−N2, 92.51(9); N1−Fe1−N3, 158.01(9); N2−Fe1−N3, 88.21(9); N1−Fe−O3, 98.75(9); N2−Fe1−O3 102.46(9); N1−Fe1−O1, 101.90(8); N3−Fe1−O1, 74.62(8); N2−Fe1−O1, 162.36(8); O3−Fe1−O1, 85.51(8)°.

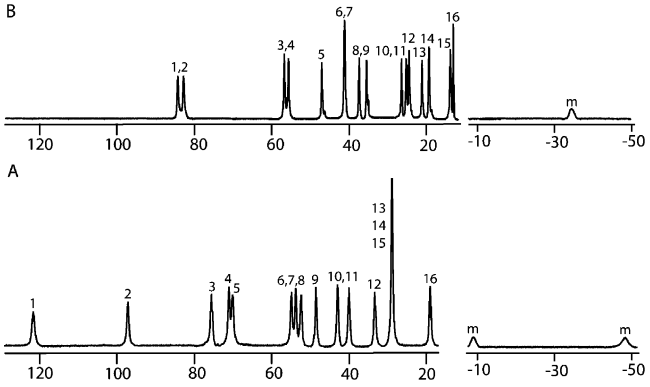

Figure 9. Portions of the 500 MHz ^{1}H NMR spectrum of the open chain tetrapyrrole complex **3** in pyridine-d_5. at: (A) 245 K and (B) 298 K.

8. The bond distances and angles in the four-coordinate form are similar.[1] As seen in Figure 8, oxidation of the porphyrin ligand has produced a linear tetrapyrrole ligand that has been opened at the meso carbon which once bore the amino group. The original amino group is no longer present. That amino group and the meso carbon atom to which it was attached have been converted into a nitrile group. Further oxidation at a second meso carbon position has introduced a new oxygen atom that is coordinated to iron. As best seen in part B of Figure 8, the terminal pyrrole ring bearing the nitrile substituent is twisted away from the iron and out of the plane of the coordinated tripyrrole portion of the ligand.

Portions of the ^{1}H NMR spectrum of **3** dissolved in pyridine-d_5 are shown in Figure 9. Trace A shows the spectrum at 245 K, while Trace B shows the spectrum at 298 K. The spectrum

shown in Trace B confirms the fact that resonances due to **3** are present in Trace B of Figure 6 and Trace C of Figure 7. At 298 K, the spectrum of **3** consists of 14 resonances of equal integrated intensity and one with twice that intensity spread over the 90−10 ppm region. This group of resonances is assigned to the methylene protons. As expected for a paramagnetic species, these resonances shift to lower field upon cooling, and resonances 6 and 7 becomes resolved, while the individual resonances at 30 ppm overlap. Within the tetrapyrrole ligand there are eight chemically distinct ethyl groups. Each methylene group is diastereotopic, since there is an asymmetric carbon at the meso carbon C15. Thus, the pattern of methylene resonances is consistent with the structure of this complex. As expected two meso hydrogen resonances have been observed at −9 and −48 ppm in the spectrum obtained at 245 K. These move downfield upon warming to 298 K. A Curie plot of the chemical shift of the meso and methylene protons of **3** graphed versus $1/T$ is given in the Supporting Information.

The Ultimate Oxidation Products, 8 and 13. The ^{1}H NMR spectra shown in Trace C of Figure 6 and Trace D of Figure 7 show that oxidation of either $ClFe^{III}$(*meso*-NH_2-OEP) or $(py)_2Fe^{II}$(*meso*-NH_2-OEP) eventually results in the formation of the same mixture of compounds. Resonances labeled 8 are assigned to the tripyrrole complex, [$(py)_2Fe^{III}$(HETP)], **8**, by comparison of these spectra with those of a sample prepared by oxidation of $(py)_2$Fe(OEPO) as reported earlier.[11] However, a prominent resonance at 81.2 ppm in Trace C of Figure 6 and Trace D of Figure 7 comes from a separate product, **13**. Further work is needed to characterize this species, but we have been able to purify **8** by crystallization so that it is free of **13**. We also note that **8** and **13** are formed from the oxidation of $(py)_2Fe^{III}$(OEPO) by dioxygen,[11] but the relative amount of **13** formed in that process is much smaller than it is in the oxidation of the amino-substituted porphyrins described here.

Discussion

Normally the porphyrin ligand is highly resistant to oxidation and is utilized to carry out a variety of biological processes in which highly oxidized iron complexes are formed. For example the resting state of horseradish peroxidase contains an iron(III) heme which reacts with hydrogen peroxide to form an observable intermediate, Compound I, that contains a ferryl ion (Fe^{IV}═O) and an oxidized porphyrin radical.[30] Green Compound I subsequently undergoes one electron reduction to form red Compound II, which contains a ferryl ion (Fe^{IV}═O) and a normal porphyrin. Compound II returns to the resting state by a second one-electron reduction. Highly oxidized hemes containing the ferryl ion are also implicated in the functioning of the cytochromes P-450.[31] To destroy unwanted heme, nature utilizes heme oxygenase, a non-heme enzyme which oxidizes heme, which is a substrate, and converts it into biliverdin, free iron ion, and carbon monoxide.[32,33] This process uses the bound heme to activate dioxygen which then attacks the porphyrin itself. Three molecules of dioxygen are utilized in the various stages of the heme disruption.

Synthetic iron(II) porphyrins are known to be reactive toward dioxygen. They can react reversibly to coordinate dioxygen[34] or may be converted into a highly reactive μ-peroxy−iron(III) dimer (PFe^{III}−O−O−Fe^{III}P) through interaction with dioxygen.[35] The direction of these reactions is determined by the availability of axial ligands. In the absence of axial ligands, the initial formation of PFe^{III}−O−O−Fe^{III}P (which can subsequently cleave to form PFe^{IV}═O) is favored,[36] but in pyridine solution a heme such as $(py)_2Fe^{II}$(OEP) is not attacked by dioxygen over a period of many hours. On the other hand, iron(III) porphyrins are generally impervious to reaction with dioxygen.[37] Oxidative processes that generate highly oxidized iron porphyrins from their iron(III) counterparts utilize stronger oxidants—peroxy acids, hydrogen peroxide, iodosyl benzene—to form ferryl, $(Fe^{IV}═O)^{2+}$, complexes.[38,39] In this context, then, it is surprising to find that pyridine solutions of $ClFe^{III}$(*meso*-NH_2-OEP) react so readily with dioxygen.

The reactions interconverting the iron complexes studied here are summarized in Scheme 3.

The oxidation process shown in Scheme 3 displays a number of remarkable features.

1. The iron(III) complex $ClFe^{III}$(*meso*-NH_2-OEP), **10**, reacts with dioxygen in pyridine solution to yield ring-cleavage products. Axial ligation again plays an important role in controlling the reactivity of this synthetic heme. The five-coordinate, high-spin complex, $ClFe^{III}$(*meso*-NH_2-OEP), is unreactive toward dioxygen in chloroform-*d*, but this complex is readily oxidized in pyridine solution where six-coordinate complexes are present. In preliminary work we have also observed that $ClFe^{III}$(*meso*-NH_2-OEP) in dichloromethane solutions containing an excess of *N*-methylimidazole undergoes oxidation upon exposure to dioxygen.

2. In pyridine solution the iron(II) complex $(py)_2Fe^{II}$(*meso*-NH_2-OEP) is consumed by dioxygen more rapidly than is the iron(III) complex, $ClFe^{III}$(*meso*-NH_2-OEP). The reaction of $(py)_2Fe^{II}$(*meso*-NH_2-OEP) with dioxygen initially produces the green radical **2** that was characterized earlier.[1,2] Green **2** is reactive toward further exposure to dioxygen. So far attempts to isolate this complex from solution by precipitation have not been successful because of its reactivity. The green radical **2** has not been observed to form directly from the iron(III) complex, $ClFe^{III}$(*meso*-NH_2-OEP).

3. In pyridine solution both $(py)_2Fe^{II}$(*meso*-NH_2-OEP) and $ClFe^{III}$(*meso*-NH_2-OEP) react with dioxygen to eventually produce the open-chain tetrapyrrole complex **3**. Although it is somewhat air sensitive, this complex is sufficiently stable to be isolated in crystalline form.[1] The structure of the open-chain tetrapyrrole complex **3**, which is shown in Figure 8, involves heme cleavage at the meso carbon that originally bore the amino substituent, conversion of that portion into a nitrile group, and further oxidation of another meso site. The end pyrrole ring

(30) Everse, J.; Everse, K. E.; Grisham, M. B. *Peroxidases in Chemistry and Biology*; CRC Press: Boca Raton, FL, 1991; Vols I and II.
(31) Sono M.; Roach M. P.; Coulter E. D.; Dawson J. H. *Chem. Rev.* **1996**, *96*, 2841.
(32) Maines, M. D. *Heme Oxygenase: Clinical Applications and Functions*; CRC Press: Boca Raton, FL, 1992.
(33) Ortiz de Montellano, P. R. *Acc. Chem. Res*. **1998**, *31*, 543.
(34) Momenteau M.; Reed C. A. *Chem. Rev*. **1994**, *94*, 659.
(35) Chin, D. H.; La Mar, G. N.; Balch, A. L. *J. Am. Chem. Soc*. **1980**, *102*, 4344.
(36) Chin, D. H.; Balch, A. L.; La Mar, G. N. *J. Am. Chem. Soc*. **1980**, *102*, 1446.
(37) An exception to this statement involves the iron(III) complexes with axial alkyl ligands which undego insertion of dioxygen to yield alkyl peroxo complexes: see Arasasingham, R. E.; Balch, A. L.; Cornman, C. R.; Latos-Grażyński, L. *J. Am. Chem. Soc*. **1989**, *111*, 4357.
(38) Groves, J. T.; Haushalter, R. C.; Nakamura, M.; Nemo, T. E.; Evans, B. J. *J. Am. Chem. Soc*. **1981**, *103*, 2884.
(39) Balch, A. L.; Latos-Grażyński, L.; Renner, M. W. *J. Am. Chem. Soc*. **1985**, *107*, 2983.

Scheme 3

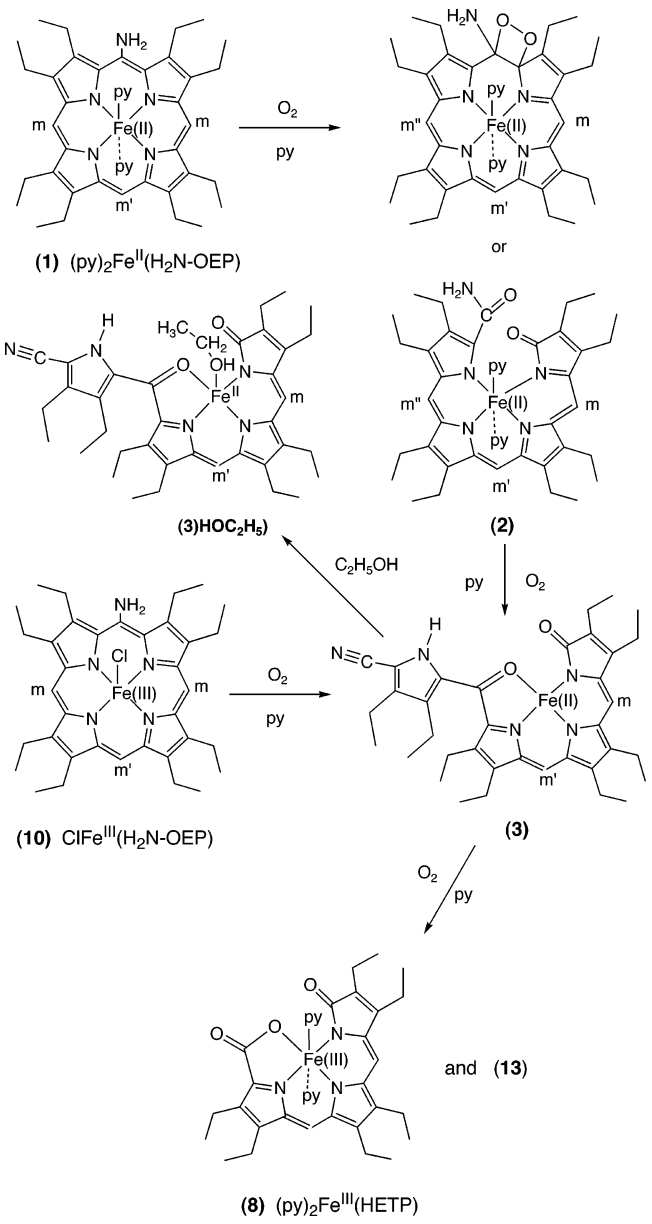

with the appended nitrile substituent is no longer coordinated to the iron center but dangles off to the side of the molecule.

4. The open-chain tetrapyrrole complex **3** is sensitive to prolonged exposure to dioxygen and is slowly (in a week) converted into a mixture of the tripyrrole complex, $(py)_2Fe^{III}$(HETP), **8**, and **13**. In the process of forming **8**, the pyrrole ring bearing the nitrile group is lost from the ligand.

Experimental Section

Materials. Octaethylporphyrin was purchased from Mid Century. *meso*-NH_2-H_2OEP was prepared by stannous chloride reduction of *meso*-NO_2-H_2OEP as described previously.[12] All solvents were used as purchased except pyridine-d_5 which was used after distillation from KOH.

$ClFe^{III}$(*meso*-NH_2-OEP). Iron was inserted in *meso*-NH_2-H_2OEP by a standard procedure under a dioxgen-free dinitrogen atmosphere to produce $ClFe^{III}$(*meso*-NH_2-OEP).[40] The solid product was redissolved in dichloromethane and washed with an aqueous 0.2 M hydrochloric acid solution. The dichloromethane solution was dried with sodium sulfate and evaporated to dryness. The product was purified by column chromatography on silica gel (3 cm × 8 cm) with 8% methanol in chloroform as an eluent. The red band was collected and evaporated to dryness; yield 90%. UV/vis spectra in chloroform, λ_{max}, nm (ϵ, M^{-1} cm^{-1}): 394 (9.8×10^4), 416 (9.3×10^4), 484 (1.1×10^4), 518 (1.1×10^4), 562 (8.0×10^3); ^{1}H NMR (chloroform-*d*, 298 K): CH_2: 52.93, 41.53, 39.63, 38.80, 35.89(2), 34.31, 33.41; NH_2: 16.39; *meso*: −85.03(*cis*), −126.76(*trans*). ^{1}H NMR (py-d_5, 298 K): for high-spin **11**: methylene: 52.70, 40.06(2), 38.86, 37.54, 36.69, 33.25(2); NH_2: 13.6; methyl: 3.80, 3.67, 1.78, 1.65; *meso*: −79.22(*cis*), −127.69(*trans*); for the low-spin **12**: methylene: 11.19, 5.08, 4.13, 1.52; NH_2: −19.15; methyl: 2.57, 2.42, 1.79, 1.67; *meso*: −60.03(*cis*), −65.99(*trans*).

Table 1. Crystallographic Data for $ClFe^{III}$(*meso*-NH_2-OEP)·0.5 $CHCl_3$·0.5 Methylcyclopentane

formula	$C_{39.5}H_{51.5}Cl_{2.5}FeN_5$
formula weight (g•mol^{-1})	740.83
color and habit	red block
crystal system	triclinic
space group	$P\bar{1}$
a, Å	10.638(2)
b, Å	12.246(2)
c, Å	14.855(3)
α, deg	90.151(4)
β, deg	96.881(4)
γ, deg	97.954(4)
V, $Å^3$	1902.3(6)
Z	2
T, K	90(2)
d_{calcd}, g cm^{-3}	1.293
radiation, (λ Å)	Mo Kα 0.71073
μ, mm^{-1}	0.607
range of transmission factors	0.82 to 0.95
R1[a]	0.055
wR2[b]	0.155

[a] $R1 = \sum||F_o| - |F_c||/\sum|F_o|$. [b] $wR2 = [\sum[w(F_o^2 - F_c^2)^2]/\sum[w(F_o^2)^2]]^{1/2}$.

K[(CN)2Fe^{III}(*meso*-NH_2-OEP)]. In a dinitrogen-filled glovebox, a methanol-d_4 solution of $ClFe^{III}$(*meso*-NH_2-OEP) (2−3 mmol) was placed in an NMR tube and carefully sealed with a rubber septum. A saturated solution of potassium cyanide in methanol-d_4 was injected into the solution. An immediate color change from red to brown was observed. The progress of the reaction is followed by ^{1}H NMR spectroscopy. ^{1}H NMR (methanol-d_4, 298 K): methylene: 5.21, 4.71, 4.60, 3.4; for NH_2: 4.25; methyl: 3.13, 2.71, 2.66, 2.55; *meso*: −51.75(*cis*), −55.52(*trans*).

Isolation of the Open-Chain Tetrapyrrole Complex 3. A 25.0 mg (0.039 mmol) sample of $ClFe^{III}$(*meso*-NH_2-OEP), **10**, was dissolved in 50 mL of pyridine. The dark-brown solution was stirred for 12 h under a stream of dioxygen. The deep-purple solution was filtered and evaporated to dryness in a vacuum. The brown solid was redissolved in a minimum volume of pyridine under a dioxygen-free dinitrogen atmosphere. Addition of dioxygen-free ethanol produced brown crystals of **3**: yield, 18.8 mg; 72%. UV/vis spectrum in pyridine: λ_{max}, nm (ϵ, M^{-1} cm^{-1}): 316 (1.1×10^5), 410 (2.5×10^4), 550 (1.0×10^4), 654 (7.0×10^3). MALDI mass spectrum (negative ion mode), 632, M^{-1}. IR, ν(CN), 2211 cm^{-1}.

Preparation of Samples for Monitoring by ^{1}H NMR Spectroscopy. In a dinitrogen filled glovebox, a red pyridine-d_5 solution of $(py)_2Fe^{II}$(*meso*-NH_2-OEP) (2−3 mmol) was placed in an NMR tube and carefully sealed with a rubber septum. The tube was removed from the glovebox, and dry dioxygen was passed through the headspace at 22 °C for 30 s via a needle. The needle was removed, and the sample was shaken to mix the contents. An immediate change of color from red to green occurred. The ^{1}H NMR spectrum of the sample was acquired. Subsequently, the tube was kept with further addition of dioxygen. The sample slowly turned greenish brown and further ^{1}H

(40) Alder, A. D.; Lango, F. R.; Kampas, F. *J. Inorg. Nucl. Chem.* **1970**, *32*, 2443.

NMR spectra were acquired over time. A similar procedure was applied to examine the behavior of $ClFe^{III}$(*meso*-NH_2-OEP). A dark-brown pyridine-d_5 solution of $ClFe^{III}$(*meso*-NH_2-OEP) was prepared under dioxygen-free conditions. After exposure to dioxygen, the color of this sample changed slowly to deep-purple and then greenish brown on standing at 22 °C.

X-ray Data Collection for $ClFe^{III}$(*meso*-NH_2-OEP)·0.5 $CHCl_3$·0.5 Methylcyclopentane. Crystals were grown by slow diffusion of methylcyclopentane into a chloroform solution of the complex. The crystal was coated with a light hydrocarbon oil and mounted in the 90 K dinitrogen stream of a Bruker SMART 1000 diffractometer equipped with CRYO Industries low-temperature apparatus. Intensity data were collected using graphite monochromated Mo Kα radiation. Crystal data are given in Table 1.

Solution and Structure Refinement. Scattering factors and correction for anomalous dispersion were taken from a standard source.[41] An absorption correction was applied.[42] The solution of the structure was obtained by direct methods with SHELXS-97 and subsequent cycles of least-squares refinement on F^2 with SHELXL-97.

(41) *International Tables for Crystallography*; Kluwer Academic Publishers: Dordrecht, The Netherlands, 1992.
(42) Sheldrick, G. M. SADABS 2.0, 2000.

Instrumentation. ^{1}H NMR spectra were recorded on a Bruker Avance 500 FT spectrometer (The ^{1}H frequency is 500.13 MHz). The spectra were recorded over a 100-kHz bandwidth with 64 K data points and a 5-ms 90° pulse. For a typical spectrum between 500 and 1000 transients were accumulated with a 50-μs delay time. The residual ^{1}H resonances of the solvents were used as a secondary reference.

Acknowledgment. We thank the NIH (Grant GM-26226, A.L.B.) and the Foundation for Polish Science (L.L.G.) for financial support, the NSF (Grant OSTI 97-24412) for partial funding of the 500 MHz NMR spectrometer, and Sigma Xi for a Grants in Aid of Research to H.K.

Supporting Information Available: Figure S1, a plot of chemical shift versus 1/*T* for the open-chain tetrapyrrole complex **3** (PDF). X-ray crystallographic files in CIF format for $ClFe^{III}$(*meso*-NH_2-OEP). This material is available free of charge via the Internet at http://pubs.acs.org.

JA0384431